Sensing and Recognition for Multiple Primary Power Level Scenario with Noise Uncertainty

Chen Qian, Feifei Gao, Han Qian, and

Abstract

In this paper, we consider the spectrum sensing in the cognitive radio (CR) scenario where the primary user (PU) transmits by multiple power levels and the noise power is uncertain. The target for secondary users (SU) is not only to detect the presence of PU, as did in the conventional "on-off" CR, but also to identify the PU's transmitting power level. With the aid of the generalized likelihood ratio test (GLRT), we prove that the energy detection (ED) is still the optimal detection technique. We also derive the closed-form decision thresholds as well as the corresponding analytical performance expression. Interestingly, a unique phenomenon called power ambiguities arises in the considered scenario which demands for careful investigation. Moreover, the SNR wall in the conventional binary CR also exists but demands for much complicated definition. We show that SNR wall in MPTP scenario XXXXXXXXXXXXXXX. To make the discussion completely, we also propose a cooperative spectrum sensing scheme that requires combination of non-binary decisions from different SUs and derive the corresponding analytical performance expression. In the end, we validate our study through various numerical results.

Index Terms

Spectrum sensing, multiple primary transmit power (MPTP), noise uncertainty, SNR wall, majority rule.

C. Qian is with Beijing University of Posts and Telecommunicaitons, Beijing, P. R. China (email: qianchen94era@bupt.edu.cn)

F. Gao and H. Qian are with Department of Automation, Tsinghua University, State Key Lab of Intelligent Technologies and Systems, Tsinghua National Laboratory for Information Science and Technology (TNList) Beijing, P. R. China (email: feifeigao@ieee.org).

I. Introduction

Cognitive radio (CR) is a promising technology to solve the spectrum scarcity problem and to cope with the inefficient spectrum usage [1]. A secondary (unlicensed) user (SU) is allowed to access the spectrum licensed to a primary user (PU) when PU is absent or when the interference to PU is below an acceptable threshold. Naturally, spectrum sensing that can detect the vacant spectrum becomes the key technology of CR [2]. The most commonly used spectrum sensing techniques include matched filter detection [3], [4], energy detection [5], and cyclostationary detection [6]. Matched filter detection is the optimal when PU's signals are perfectly known to SU; Energy detection requires least prior information about the PU's signal and is widely studied because of its lower complexity; Cyclostationary detection requires primary signal to possess cyclic features but is of high complexity and needs a large number of samples to formulate the cyclostationarity behavior.

One important assumption of these sensing methods is that PU is either idle or transmitting with a constant power, which makes the task of spectrum sensing as detecting the binary status of PU. However, it is immediately seen from many current standards, e.g., IEEE 802.11 series, GSM, and the future standards, e.g., LTE, LTE-A that the licensed users could and should be working under different transmit power levels in order to cope with different situations. The spectrum sensing problem when PU has multiple transmit power levels (MPTP) was recently investigated in [**?**], where both the PU's on-off status as well as the PU's power levels could be recognized. It was also demonstrated in [15] that by detecting the multiple power levels of PU, SU could improve the power allocation strategy and achieve much higher throughput than mistakenly assuming binary status of PU.

One the other hand, many conventional sensing works also assume perfect knowledge of noise variance. However, in a practical system the noise variance cannot be perfectly measured due to initial calibration error, temperature variation, changes in low noise amplifier gain by thermal variation, and interference, etc [25]. Noise uncertainty has negative effects on the precision of spectrum sensing and sometimes even fails the sensing. Such influence has been studied in several works, including [**?**], [17], [16], [17] [8], [10], [11]. In [8], the authors studied the fundamental limits on energy detection in low signal-to-noise ratio (SNR) under noise uncertainty. Following this work, [9] designed energy detectors based on various types of noise uncertainty models, and [10], [11] proposed several spectrum sensing methods using the generalized likelihood ratio test (GLRT) when signals, noise and channels contain uncertainty. Especially, Tandra and Sahai [25] found that when the signal-to-noise ratio (SNR) is lower than a certain value, the performance of PU detection cannot be optimized by increasing the sensing time. This interesting phenomena is well known as signal-to-noise ratio (SNR) wall and has attract much attention [18], [19].

In this paper, we study the spectrum sensing in MPTP scenario considering the noise uncertainty at the secondary user (SU) side. With multiple hypotheses testing and GLRT, we first prove that the energy detection is still the optimal for both PU detection and power level recognition. However, we point that the uncertain noise power would bring a new and unique phenomenon in MPTP scenario, named as *power ambiguity*. We the carefully investigate the effect of power ambiguity and derive the closed-form solutions for the decision region. The corresponding closed-form decision probabilities are also computed. Similar to binary sensing [25], SNR wall effect also exist for MPTP scenario but with modified definition. Different from the binary case, in MPTP scenario there existing two SNR walls for each power level, one on each side. We further derive the exact position of these SNR walls. To make the proposed study complete, we propose a cooperative sensing scheme based on a modified majority law due to the power ambiguity effect. XXXXXXXXXXXX łłXXXXXXXXXXXX Finally, simulating results are provided to corroborate the proposed studies.

The rest of this paper is organized as follows. In Section II, we describe the CR model in MPTP scenario and formulate the spectrum sensing problem as a composite multiple hypotheses problem. In Section III, we design the sensing and recognition algorithm and derive the decision regions as well as the decision probability. In the same section, the power ambiguity and the SNR wall phenomena are investigated. In Section IV, we propose a cooperative sensing scheme based on the majority law and derived its analytical performance expression. Simulation results are provided in Section V and conclusions are made in Section VI.

II. System Descriptions

A. Signal Model

Consider a simple CR network with a pair of PU and SU, where PU could either be absent or operating under any power level $P_k, k \in \{1, 2, \ldots, M\}$ satisfying $P_{k+1} > P_k > 0, \forall k$. To unify the notation, we define $P_0 = 0$ as power when PU is absent. The received signal at SU is given by

$$\mathcal{H}_k : x_n = \sqrt{P_k}\sqrt{\gamma}e^{j\phi}s_n + \omega_n, \quad k = 0, \cdots, M, \tag{1}$$

where $\mathcal{H}_k$ denotes the hypothesis that PU is operating under power level P_k; s_n denotes the n-th sample transmitted from PU which follows circularly symmetric complex Gaussian (CSCG) distribution with zero mean and unit variance; $\sqrt{\gamma}$ is the channel gain and ϕ is the channel phase; ω_n denotes the additive white Gaussian noise with zero mean and variance σ^2.

Hence, x_n also follows CSCG distribution, i.e.

$$x_n|\mathcal{H}_k \sim \mathcal{CN}(0, P_k\gamma + \sigma^2), \quad \forall \mathcal{H}_k. \tag{2}$$

Define $\Pr(\mathcal{H}_k)$ as the prior probability of the state PU is operating under power P_k. Then the presence state of PU is denoted as $\mathcal{H}_{\text{on}} = \bigcup_{k=1}^{M} \mathcal{H}_k$, and the prior probability of $\mathcal{H}_{\text{on}}$ is $\Pr(\mathcal{H}_{\text{on}}) = \sum_{k=1}^{M} \Pr(\mathcal{H}_k)$. While the absence state of PU can also be defined $\mathcal{H}_{\text{off}} = \mathcal{H}_{\text{on}}$ and has the prior probability $\Pr(\mathcal{H}_{\text{off}}) = \Pr(\mathcal{H}_0)$.

Similar to [20], we here make the following assumptions:

1) SU has knowledge power levels $\{P_0, P_1, \cdots, P_M\}$ as they are normally the deterministic values regulated by the standards.
2) We assume that the channel gain $\sqrt{\gamma}$ is known at SU while the phase ϕ can be unknown.[1]

[1]Some energy detection algorithms [?], [29], [30] assume AWGN channel, which is the equivalent to assuming $\sqrt{\gamma} = 1$. Nevertheless, a new result that could release the necessities of channel information and PU's power level information was recently published in [31].

B. Noise Uncertainty

Noise is an aggregation of various sources, among which four factors mainly contribute to the noise power uncertainty [21]: initial calibration error, temperature variation, changes in low noise amplifier gain due to the thermal variation, and interferers. The uncertainty caused by calibration error and thermal variation can be overcome by noise power estimation because thermal changes slowly. Indeed this part of the noise power is typically stationary for a few minutes [22]. However, the interference from other SUs or other opportunistic systems changes too fast to be tracked with periodical estimations. This dynamic background RF energy causes noise uncertainty in CR systems, i.e., σ^2 in system (1) is unknown.

III. Sensing and Recognition Algorithm

Suppose that SU receives a total number of N samples during a sensing period, and define $\mathbf{x} = [x_1, x_2, \cdots, x_N]^T$, $\mathbf{s} = [s_1, s_2, \cdots, s_N]^T$, $\mathbf{w} = [w_1, w_2, \cdots, w_N]^T$. Due to the independence in $\mathbf{s}$ and $\mathbf{w}$, the probability density function (pdf) of $\mathbf{x}$ under $\mathcal{H}_k$ is given by

$$p(\mathbf{x}|\mathcal{H}_k) = \frac{1}{[\pi(\sigma^2 + P_k\gamma)]^N} \exp\left(-\frac{\|\mathbf{x}\|^2}{\sigma^2 + P_k\gamma}\right). \tag{3}$$

The unknown noise variance leads to an employment of composite hypothesis test. Let us first apply the generalized likelihood ratio test (GLRT) [23] and obtain the maximum likelihood estimate (MLE) of σ^2 under $\mathcal{H}_k$ as

$$\hat{\sigma}_k^2 = \arg\max_{\sigma_k^2} p(\mathbf{x}|\mathcal{H}_k, \sigma_k^2) = \arg\max_{\sigma_k^2} \frac{1}{[\pi(\sigma_k^2 + P_k\gamma)]^N} \exp\left(-\frac{\|\mathbf{x}\|^2}{\sigma_k^2 + P_k\gamma}\right). \tag{4}$$

Considering that σ^2 must be a positive value, the MLE of σ^2 is derived as

$$\hat{\sigma}_k^2 = (T(\mathbf{x}) - P_k\gamma)^+, \tag{5}$$

where $(\cdot)^+$ denotes $\max\{0, \cdot\}$, and $T(\mathbf{x}) \triangleq \|\mathbf{x}\|^2/N$ represents the mean energy of the received samples.

To find the most possible power level of PU, we use GLRT to compare each hypothesis pair $(\mathcal{H}_i, \mathcal{H}_j), \forall i, j \in \{0, 1, \cdots, M\}$

$$\xi_{i,j}(\mathbf{x}) = \frac{p(\mathbf{x}|\mathcal{H}_i, \hat{\sigma}_i)}{p(\mathbf{x}|\mathcal{H}_j, \hat{\sigma}_j)} \underset{\mathcal{H}_j}{\overset{\mathcal{H}_i}{\gtrless}} 1. \tag{6}$$

For multiple hypotheses $\mathcal{H}_k$, the decision of the PU's power level with GLRT method applied should be

$$\hat{k} = \arg \max_{i \in \{0,1,\cdots,M\}} p(\mathbf{x}|\mathcal{H}_k, \hat{\sigma}_k^2). \tag{7}$$

A. Fully Unknown Noise Power

Let us first consider the case when SU has no knowledge of noise variance. Without loss of generality, assume the received $T(\mathbf{x})$ stays between the value of $P_m\gamma$ and $P_{m+1}\gamma$ for a certain m, i.e., $P_0\gamma < \cdots < P_m\gamma < T(\mathbf{x}) < P_{m+1}\gamma < \cdots < P_M\gamma$. Then, the estimation (5) can be expanded as

$$\hat{\sigma}_k^2 = \begin{cases} T(\mathbf{x}) - P_k\gamma, & k = 0, 1, \ldots, m \\ 0, & k = m+1, \ldots, M, \end{cases}$$

and the corresponding pdf is

$$p(\mathbf{x}|\mathcal{H}_k, \hat{\sigma}_k^2) = \begin{cases} \dfrac{1}{(\pi T(\mathbf{x}))^N} \exp(-N), & 0 \le k \le m \\ \dfrac{1}{(\pi P_k\gamma)^N} \exp\left(-\dfrac{N}{P_k\gamma} T(\mathbf{x})\right), & m+1 \le k \le M. \end{cases} \tag{8}$$

It is seen that all the $m+1$ hypotheses $\mathcal{H}_0, \mathcal{H}_1, \ldots, \mathcal{H}_m$ share the same likelihood pdf.

Since $T(\mathbf{x}) < P_{m+1}\gamma$, it can be readily check that $p(\mathbf{x}|\mathcal{H}_0, \hat{\sigma}_0^2) = \ldots = p(\mathbf{x}|\mathcal{H}_m, \hat{\sigma}_m^2)$ are the maximum pdf among all $p(\mathbf{x}|\mathcal{H}_k, \hat{\sigma}_k^2), k \in \{0, 1, \cdots, M\}$. Hence, the detection decision contains $m+1$ hypotheses.

Definition 1: If the decision include more than one hypothesises, we call this phenomenon as *power ambiguity*.

Remark 1: Power ambiguity is a unique phenomenon for MPTP scenario with unknown noise variance and does not exist for the conventional binary spectrum sensing. Interestingly, another unique phenomenon for MPTP scenario with known noise variance is identified as *power mask* [20], where some power levels hide below other power levels. Nevertheless, power mask effect does not exist when the noise variance is unknown.

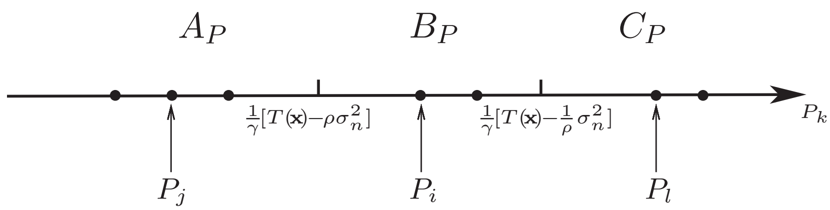

Fig. 1. Distribution of P_k for a given $T(\mathbf{x})$.

B. Noise Uncertainty Restriction

Practically, a stationary noise power can be estimated by taking a large number of samples, while some residual uncertainty caused by interference still exists. For this reason, one may treat the noise power as ranging from a lower bound to an upper bound [11]. We then adopt the uncertainty model from [25] and assume the value of σ^2 belongs to $[(1/\rho)\sigma_0^2, \rho\sigma_0^2]$, where σ_0^2 denotes the nominal noise variance and $\rho > 1$ is a parameter that quantifies the size of uncertainty.

With the constraint $(1/\rho)\sigma_0^2 \leqslant \sigma^2 \leqslant \rho\sigma_0^2$, the MLEof σ^2 under hypothesis $\mathcal{H}_k$ is recomputed from (4) as

$$\hat{\sigma}_k^2 = \min\{\max\{(1/\rho)\sigma_0^2, T(\mathbf{x}) - P_k\gamma\}, \rho\sigma_0^2\}. \tag{9}$$

Let us then define the sets: $A_P \triangleq \{k|P_k\gamma < T(\mathbf{x}) - \rho\sigma_0^2\}$, $B_P \triangleq \{k|T(\mathbf{x}) - \rho\sigma_0^2 \leqslant k\gamma \leqslant T(\mathbf{x}) - \frac{1}{\rho}\sigma_0^2\}$, and $C_P \triangleq \{P_k|P_k\gamma > T(\mathbf{x}) - \frac{1}{\rho}\sigma_0^2\}$ for a given $T(\mathbf{x})$. Fig. 1 helps illustrate the distribution of the primary power levels, where P_j, P_i and P_l are picked from three sets, representing three typical positions on the axis.

Based on the divided set, the estimation from (9) can be explicitly expressed as

$$\hat{\sigma}_k^2 = \begin{cases} \rho\sigma_n^2, & k \in A_P \\ T(\mathbf{x}) - P_i\gamma, & k \in B_P \\ \frac{1}{\rho}\sigma_n^2, & k \in C_P. \end{cases} \tag{10}$$

With (10), we obtain

$$p(\mathbf{x}|\mathcal{H}_k, \hat{\sigma}_k^2) = \begin{cases} \dfrac{1}{[\pi(P_k\gamma + \rho\sigma_n^2)]^N} \exp\left[-\dfrac{NT(\mathbf{x})}{P_k\gamma + \rho\sigma_n^2}\right], & k \in A_P, \\ \dfrac{1}{(\pi T(\mathbf{x}))^N} \exp(-N), & k \in B_P, \\ \dfrac{1}{[\pi(P_k\gamma + \frac{1}{\rho}\sigma_0^2)]^N} \exp\left[-\dfrac{NT(\mathbf{x})}{P_k\gamma + \frac{1}{\rho}\sigma_0^2}\right] & k \in C_P. \end{cases} \tag{11}$$

where $\mathcal{H}_k$'s, $k \in B_P$, share the same pdf.

To find the maximum likelihood probability $p(\mathbf{x}|\mathcal{H}_k, \hat{\sigma}_k^2)$, we compare the two hypothesis pairs $(\mathcal{H}_i, \mathcal{H}_j)$ and $(\mathcal{H}_i, \mathcal{H}_l)$ using the likelihood ratio (6), where $j \in A_P$, $i \in B_P$, $l \in C_P$.

$$\ln \xi_{i,j}(\mathbf{x}) = \frac{1}{N}\left[\ln \frac{\rho\sigma_0^2 + P_j\gamma}{T(\mathbf{x})} + \frac{T(\mathbf{x})}{\rho\sigma_0^2 + P_j\gamma} - 1\right], \tag{12}$$

$$\ln \xi_{i,l}(\mathbf{x}) = \frac{1}{N}\left[\ln \frac{\frac{1}{\rho}\sigma_0^2 + P_l\gamma}{T(\mathbf{x})} + \frac{T(\mathbf{x})}{\frac{1}{\rho}\sigma_0^2 + P_l\gamma} - 1\right]. \tag{13}$$

Since the function $f(y) = y + \ln\dfrac{1}{y}$ has the minimum value $f(1) = 1$ in the interval $(0, +\infty)$, the inequalities $\xi_{i,j}(\mathbf{x}) > 1$ and $\xi_{i,l}(\mathbf{x}) > 1$ hold regardless of the value of P_j and P_l. Hence, $\mathcal{H}_k$ with $k \in B_P$ all have the maximum likelihood probability. Once again, we cannot discriminate among these power levels, and the power ambiguity happens when B_P contains more than one power levels.

Remark 2: When power ambiguity happens, the experiment is deemed as failed. In another word, any experiment with a $T(\mathbf{x})$ falling in any overlapping area is considered as failure.

We next compute the decision regions of different hypotheses and proceed with the following two cases:

Case 1: The set B_P being nonempty: In this case, the necessary condition for hypothesis $\mathcal{H}_i$ to be selected is to stay in set B_P, i.e., $T(\mathbf{x}) - \rho\sigma_0^2 < P_i\gamma < T(\mathbf{x}) - \frac{1}{\rho}\sigma_0^2$, or equivalently $T(\mathbf{x}) \in (P_i\gamma + \sigma_0^2/\rho, P_i\gamma + \rho\sigma_0^2)$. This interval is named as the *potential decision region* (PDR) for hypothesis $\mathcal{H}_i$ because the final decision has not been made yet. Let us define PDR for all power level $P_k, k \in \{0, 1, \cdots, M\}$ as

$$\mathcal{R}_1(\mathcal{H}_k) = (P_k\gamma + \sigma_0^2/\rho, P_k\gamma + \rho\sigma_0^2) = (\phi_{lk}, \phi_{uk}), \tag{14}$$

where ϕ_{lk} and ϕ_{uk} are the corresponding items.

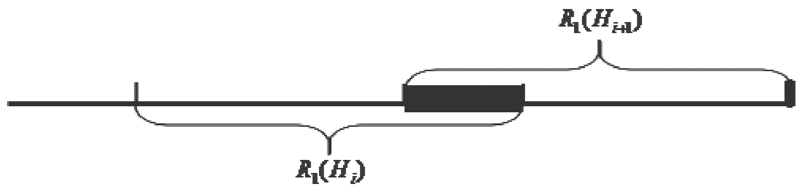

Fig. 2. A possible distribution of PDR for $\mathcal{H}_i$ and $\mathcal{H}_{i+1}$.

Randomly pick two indices $i, j \in \{0, 1, \cdots, M\}$. If for any (i, j) pair $\mathcal{R}_1(\mathcal{H}_i)$ and $\mathcal{R}_1(\mathcal{H}_j)$ do not overlap, then we could claim that under no situations would B_P contains more than one power level. In another word, power ambiguity never happens. Thus, $\mathcal{R}_1(\mathcal{H}_i)$ serves as the decision regions for hypothesis $\mathcal{H}_i$.

However, the distribution of PDR for different power levels might look like Fig. 2, where $\mathcal{R}_1(\mathcal{H}_i)$ and $\mathcal{R}_1(\mathcal{H}_{i+1})$ have overlapping areas. If $T(\mathbf{x})$ falls inside the black square region in Fig. 2, then both P_i or P_{i+1} would be contained in B_P. Thus, one cannot tell whether P_i or P_{i+1} has the preference over the other since power level contained in B_P share the same likelihood, resulting into power ambiguity. The boundary of this overlapping area is computed as $(\phi_{l(i+1)}, \phi_{ui}) = (P_{i+1}\gamma + \frac{1}{\rho}\sigma_0^2, P_i\gamma + \rho\sigma_0^2)$. On the other side, if $T(\mathbf{x})$ falls into the part of $\mathcal{R}_1(\mathcal{H}_k)$ that does not overlap with any other PDR, then the recognition result is uniquely P_k and there is no power ambiguity. In general, if B_P consists of $P_i, P_{i+1}, \cdots, P_{i+m}$, the overlapping area of PDR is

$$T(\mathbf{x}) \in (\phi_{l(i+m)}, \phi_{ui}) = (P_{i+m}\gamma + \sigma_0^2/\rho, P_i\gamma + \rho\sigma_0^2). \tag{15}$$

Note that the interval in (15) is valid only when $(\rho - 1/\rho)\dfrac{\sigma_0^2}{\gamma} > P_{i+m} - P_i$ holds for true.

Now, let us formulate the decision region for Case *I*:

$$\mathcal{DR}_1(\mathcal{H}_i) = (\max(P_i + \frac{\sigma_0^2}{\rho}, P_{i-1} + \rho\sigma_0^2), \min(P_i + \rho\sigma_0^2, P_{i+1} + \frac{\sigma_0^2}{\rho}))) \tag{16}$$

Where $\mathcal{DR}$ stands for decision region.

Case II: The set B_P being empty: In this case, since no power level is contained in $(T(\mathbf{x}) - \rho\sigma_0^2, T(\mathbf{x}) - \frac{1}{\rho}\sigma_0^2)$, there must be an $m \in \{0, 1, \cdots, M-1\}$ satisfying $P_m\gamma < T(\mathbf{x}) - \rho\sigma_0^2 <$

$T(\mathbf{x}) - \frac{1}{\rho}\sigma_0^2 < P_{m+1}\gamma$. Simple transformation yields: $P_m\gamma + \rho\sigma_0^2 < T(\mathbf{x}) < P_{m+1}\gamma + \frac{1}{\rho}\sigma_0^2$. Since B_P is empty, the MLE of σ^2 is simplified to

$$\hat{\sigma}_k^2 = \begin{cases} \rho\sigma_0^2, \quad k = 0, 1, \ldots, m & \text{(17a)} \\ \dfrac{1}{\rho}\sigma_0^2, \quad k = m+1, \ldots, M, & \text{(17b)} \end{cases}$$

which upon substitution into the likelihood pdf yields

$$p(\mathbf{x}|\mathcal{H}_k, \hat{\sigma}_k^2) = \begin{cases} \dfrac{1}{[\pi(P_k\gamma + \rho\sigma_0^2)]^N} \exp\left(-\dfrac{NT(\mathbf{x})}{P_k\gamma + \rho\sigma_n^2}\right) \quad k = 0, 1, \ldots, m, & \text{(18a)} \\ \dfrac{1}{[\pi(P_k\gamma + \frac{1}{\rho}\sigma_n^2)]^N} \exp\left(-\dfrac{NT(\mathbf{x})}{P_k\gamma + \frac{1}{\rho}\sigma_n^2}\right) \quad k = m+1, \ldots, M & \text{(18b)} \end{cases}$$

Considering the monotonicity of function $h(y) = \dfrac{1}{y^N}\exp(-Na/y)$ and the condition $P_0\gamma + \rho\sigma_n^2 < \ldots < P_m\gamma + \rho\sigma_n^2 < T(\mathbf{x}) < P_{m+1}\gamma + \frac{1}{\rho}\sigma_n^2 < \ldots < P_M\gamma + \frac{1}{\rho}\sigma_n^2$, (18a) has the maximum when $k = m$, and (18b) has the maximum when $k = m+1$. Then, we only need to compare the hypothesis pair $(\mathcal{H}_{m+1}, \mathcal{H}_m)$, whose likelihood ratio is given by

$$\frac{1}{N}\ln\xi_{m+1,m}(\mathbf{x}) = T(\mathbf{x})\frac{(\sigma_0^2/\rho + P_{m+1}\gamma) - (\rho\sigma_0^2 + P_m\gamma)}{(\sigma_0^2/\rho + P_{m+1}\gamma)(\rho\sigma_0^2 + P_m\gamma)} + \ln\frac{\rho\sigma_0^2 + P_m\gamma}{\sigma_0^2/\rho + P_{m+1}\gamma}.$$

Hence we obtain the detection threshold as

$$T(\mathbf{x}) \underset{\mathcal{H}_m}{\overset{\mathcal{H}_{m+1}}{\gtrless}} \frac{(\sigma_0^2/\rho + P_{m+1}\gamma)(\rho\sigma_0^2 + P_m\gamma)}{(\sigma_0^2/\rho + P_{m+1}\gamma) - (\rho\sigma_0^2 + P_m\gamma)} \ln\frac{\sigma_0^2/\rho + P_{m+1}\gamma}{\rho\sigma_0^2 + P_m\gamma}.$$

Let us define $\mathcal{R}_2(\mathcal{H}_k)$ here in correspondence to $\mathcal{R}_1(\mathcal{H}_k)$.

$$\mathcal{R}_2(\mathcal{H}_k) = (\theta_k, \theta_{k+1}), \tag{19}$$

where θ_k is defined in (20).

Since there is no power ambiguity in Case *II*, $\mathcal{R}_2(\mathcal{H}_k)$ directly functions as the decision region, i.e. $\mathcal{DR}_2(\mathcal{H}_i) = \mathcal{R}_2(\mathcal{H}_k)$.

$$\theta_k = \begin{cases} 0, & k = 0 \\ \dfrac{(\sigma_0^2/\rho + P_k\gamma)(\rho\sigma_0^2 + P_{k-1}\gamma)}{(\sigma_0^2/\rho + P_k\gamma) - (\rho\sigma_0^2 + P_{k-1}\gamma)} \ln\dfrac{\sigma_0^2/\rho + P_k\gamma}{\rho\sigma_0^2 + P_{k-1}\gamma}, & k = 1, 2, \cdots, M \\ +\infty, & k = M+1. \end{cases} \tag{20}$$

We next check the relationship between $\mathcal{R}_1(\mathcal{H}_k)$ and $\mathcal{R}_2(\mathcal{H}_k)$.

<u>Lemma</u> 1: Mathematically, $\mathcal{R}_1(\mathcal{H}_k)$ and $\mathcal{R}_2(\mathcal{H}_k)$ in Case *I* and Case *II* satisfy $\mathcal{R}_1(\mathcal{H}_k) \subseteq \mathcal{R}_2(\mathcal{H}_k)$.

Proof: It is known:

$$f_1(y) = \ln y + \frac{1}{y} > f_1(1) = 1, \forall y \neq 1 \tag{21}$$

$$f_2(y) = \ln y - y < f_2(1) = -1, \forall y \neq 1, \tag{22}$$

Substituting $y = \dfrac{P_k\gamma + \sigma_n^2/\rho}{P_{k-1}\gamma + \rho\sigma_n^2}$ into (21) and (22) yields $\theta_k > P_{k-1}\gamma + \rho\sigma_n^2$, $\theta_k < P_k\gamma + \sigma_n^2/\rho$ respectively, i.e. $\theta_k < \phi_{lk}$ and $\theta_{k+1} > \phi_{uk}$. ■

Pay attention to this proof is under the condition that power ambiguity between P_{k-1} and P_k does not exist, i.e. $(\sigma_0^2/\rho + P_k\gamma) - (\rho\sigma_0^2 + P_{k-1}\gamma) > 0$. When $(\sigma_0^2/\rho + P_k\gamma) - (\rho\sigma_0^2 + P_{k-1}\gamma) \leq 0$, the conclusion would be totally different in that $\theta_k > \phi_{lk}$ and $\theta_{k+1} < \phi_{uk}$. The corresponding proof is eliminated as it is similar to that of Lemma 1.

To systematically combine conclusion derived from Case *I* and Case *II*, let us make a simple summation. Above all, it worth note that we remove the applicable condition for $\mathcal{R}_1(\mathcal{H}_k)$ and $\mathcal{R}_2(\mathcal{H}_k)$ here, but only reserve their mathematical form. The analysis goes as the follows:

For each $k \in \{0, 1, \cdots, M\}$, there exists a corresponding $\mathcal{R}_1(\mathcal{H}_k)$. Any $T(\mathbf{x})$ falling in $\mathcal{R}_1(\mathcal{H}_k)$ would lead to the result that hypothesis $\mathcal{H}_i$ wins over others since it leads to the conclusion that $P_k \in B_P$. When noise uncertainty is minor, i.e. ρ is not far from 1, no overlapping areas exist for any $\mathcal{R}_1(\mathcal{H}_i)$ and $\mathcal{R}_1(\mathcal{H}_j)$. Meanwhile, the summation of all $\mathcal{R}_1(\mathcal{H}_k)$ cannot include all possible values of $T(\mathbf{x})$, leaving vacant regions between neighboring $\mathcal{R}_1(\mathcal{H}_k)$ as shown in the first figure in Fig. 3. It has been proved before that $\mathcal{R}_1(\mathcal{H}_k) \subseteq \mathcal{R}_2(\mathcal{H}_k)$. And combining the prior discussion in Case *I* and Case *II*, it naturally yields the conclusion that the decision region for $\mathcal{H}_k$ is $\mathcal{R}_2(\mathcal{H}_k)$ in this case.

Visually, the width of $\mathcal{R}_1(\mathcal{H}_k)$ is under the control of ρ, whose value represents the size of nosie uncertainty. With ρ gets larger, or say noise uncertainty becomes severer, some pairs of $\mathcal{R}_1(\mathcal{H}_i)$ and $\mathcal{R}_1(\mathcal{H}_j)$ would overlap gradually. This procedure is like the extension of water wave, where the approximate wave overlap first. For demonstration, let us consider the case where $\mathcal{R}_1(\mathcal{H}_k)$ and $\mathcal{R}_1(\mathcal{H}_{k+1})$ overlap but $\mathcal{R}_1(\mathcal{H}_k)$ and $\mathcal{R}_1(\mathcal{H}_{k-1})$ do not. In this case, $\mathcal{R}_2(\mathcal{H}_k)$

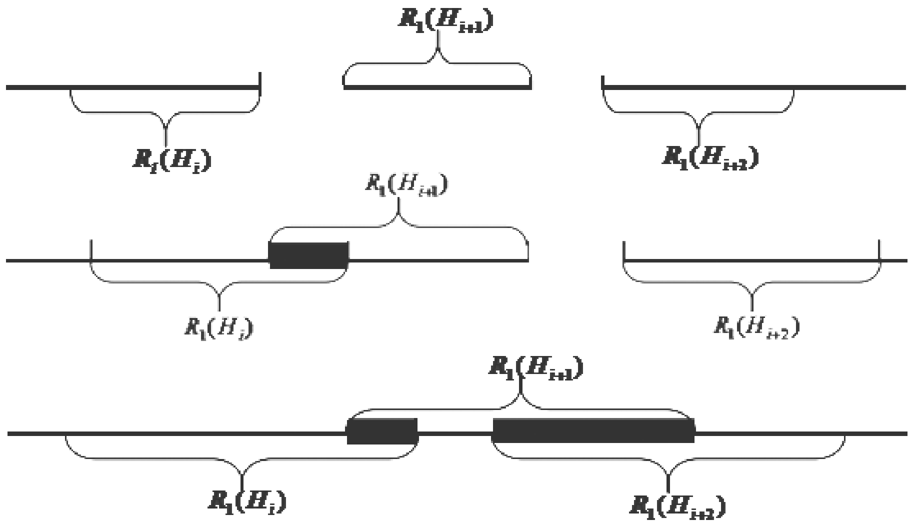

Fig. 3. Three different distributions of $\mathcal{R}_i(\mathcal{H}_i)$, $\mathcal{R}_i(\mathcal{H}_{i+1})$ and $\mathcal{R}_i(\mathcal{H}_{i+2})$.

no longer function as the decision region as $T(\mathbf{x})$ falling in $(\phi_{l(k+1)}, \phi_{u(k)})$ (the black region in the second figure in Fig. 3 cannot get distinguished properly due to power ambiguity. Thus, with the right boundary amended, the decision region for $\mathcal{H}_k$ is $[\theta_k, \phi_{l(k+1)})$.

Then, an even larger ρ would make $\mathcal{R}_1(\mathcal{H}_k)$ and $\mathcal{R}_1(\mathcal{H}_{k-1})$ overlap too, as shown in the third picture in Fig. 3. Skipping the similar analysis, we directly give the conclusion: the decision region for $\mathcal{H}_k$ is $[\phi_{u(k-1)}, \phi_{l(k+1)})$.

Finally, we propose the following theorem,

Theorem 1: The decision region for $\mathcal{H}_k$ is:

$$\mathcal{DR}(\mathcal{H}_k) = (\theta_k, \theta_{k-1}] - \left[\theta_k, \max(\theta_k, \phi_{u(k-1)})\right] - \left[\min(\theta_{k+1}, \phi_{l(k+1)}), \theta_{k+1}\right] \tag{23}$$

Now, let us propose the recognition strategy under the restricted noise uncertainty.

C. Performance Analysis

To evaluate the performance of sensing in MPTP, we define $\Pr(\mathcal{H}_i|\mathcal{H}_j)$ as the probability of the event that the final decision is $\mathcal{H}_i$ while the actual primary transmitting power is P_j. According to [26], the test statistic $T(\mathbf{x})$ under hypothesis $\mathcal{H}_k$ approximately follows a Gaussian

Algorithm 1 Strategy for recognition in MPTP scenario

1) Compute the average energy $T(\mathbf{x}) \triangleq \frac{\|\mathbf{x}\|^2}{N}$, where $\mathbf{x}$ is the received signal.
2) Formulate the set B_P by checking $P_k\gamma \in (T(\mathbf{x}) - \rho\sigma_0^2, T(\mathbf{x}) - \frac{1}{\rho}\sigma_0^2)$. If B_P contains only one power level P_k, then the sensing ends and the decision $\mathcal{H}_k$ is made. If two or more power levels satisfy the requirement, the recognition is claimed to fail. If there is no power level in B_P, then proceed to the next step.
3) Compute all (θ_i, θ_{i+1}). If $T(\mathbf{x})$ belongs to (θ_k, θ_{k+1}), then the decision $\mathcal{H}_i$ is made.

distribution for a large N. The corresponding mean and variance are computed as $\mu_t = P_k\gamma + \hat{\sigma}_k^2$ and $\sigma_t^2 = \frac{1}{N}(P_k\gamma + \hat{\sigma}_k^2)^2$, respectively. Thus, the pdf of $T(\mathbf{x})$ is given by

$$p(t|\mathcal{H}_k) = \frac{\sqrt{N}}{\sqrt{2\pi}(P_k\gamma + \hat{\sigma}_k^2)} \exp\left(-\frac{N(t - P_k\gamma - \hat{\sigma}_k^2)^2}{2(P_k\gamma + \hat{\sigma}_k^2)^2}\right).$$

Corresponding to the second step in algorithm 1, we compute the probability of power ambiguity. Though power ambiguity could occur among more than two power levels, we will focus on the ambiguity between only two power levels. The extension to the ambiguity among more than two power levels can be straightforwardly achieved with tedious discussion and is thus omitted.

Here we define a function $f(x)$ to facilitate following discussion:

$$f(x) = \begin{cases} x & x > 0 \\ 0 & x \leqslant 0 \end{cases} \tag{24}$$

Let us define the probability of the ambiguity between P_i and P_{i+1} when PU actually transmits with power level P_j:

$$\begin{aligned} &\Pr(\mathcal{A}_{i,i+1}|\mathcal{H}_j) = f\left(\Pr\{\phi_{l(i+1)} < T(x) \leqslant \phi_{ui}|\mathcal{H}_j\}\right) \\ &= f\left(\mathcal{Q}\left[\sqrt{N}\left(\frac{\phi_{l(i+1)}}{P_j\gamma + \hat{\sigma}_j^2} - 1\right)\right] - \mathcal{Q}\left[\sqrt{N}\left(\frac{\phi_{ui}}{P_j\gamma + \hat{\sigma}_j^2} - 1\right)\right]\right). \end{aligned} \tag{25}$$

where $\mathcal{A}_{i,i+1}$ stands for power ambiguity between $\mathcal{H}_i$ and $\mathcal{H}_{i+1}$, $\mathcal{Q}(\cdot)$ is the complementary distribution function of the standard Gaussian, and $\phi_{l(i+1)}, \phi_{u(i)}$ are given in Section III-B.

Pay attention to (25) makes sense only when $\phi_{l(i+1)} < \phi_{u(i)}$ in the consideration of power ambiguity.

Similarly, when power ambiguity does not exist, the decision probability can be computed as

$$\begin{aligned}\Pr(\mathcal{H}_i|\mathcal{H}_j, NA) &= \Pr\{\theta_i < T(x) \leqslant \theta_{i+1}|\mathcal{H}_j\}\\ &= \mathcal{Q}\left[\sqrt{N}\left(\frac{\theta_i}{P_j\gamma+\hat{\sigma}_j^2}-1\right)\right]-\mathcal{Q}\left[\sqrt{N}\left(\frac{\theta_{i+1}}{P_j\gamma+\hat{\sigma}_j^2}-1\right)\right],\end{aligned} \tag{26}$$

where NA stands for no power ambiguity.

Combining these two circumstances, the possibility of SU determining P_i when PU transmitting by P_j is derived as

$$\begin{aligned}&\Pr(\mathcal{H}_i|\mathcal{H}_j) = f\left(\Pr(\mathcal{H}_i|\mathcal{H}_j, NA) - f\left(\Pr(\mathcal{A}_{i,i+1}, \mathcal{R}_1(\mathcal{H}_i)|\mathcal{H}_j)\right) - f\left(\Pr(\mathcal{A}_{i-1,i}, \mathcal{R}_1(\mathcal{H}_i)|\mathcal{H}_j)\right)\right)\\ =&f\left(\Pr\{\theta_i < T(x) \leqslant \theta_{i+1}|\mathcal{H}_j\} - f\left(\Pr\{\phi_{l(i+1)} < T(x) \leqslant \theta_{i+1}|\mathcal{H}_j\}\right) - f\left(\Pr\{\theta_i < T(x) \leqslant \phi_{u(i-1)}|\mathcal{H}_j\}\right)\right).\end{aligned} \tag{27}$$

Then detection probability and force alarm probability can be easily obtained from the summations of the corresponding $\Pr(\mathcal{H}_i|\mathcal{H}_j)$, i.e.,

$$\begin{aligned}\mathrm{P_d} &= \frac{1}{\Pr(\mathcal{H}_{\mathrm{on}})}\sum_{i=1}^{M}\sum_{j=1}^{M}\Pr(\mathcal{H}_i|\mathcal{H}_j)\Pr(P_j)\\ \mathrm{P_{fa}} &= \sum_{i=1}^{M}\Pr(\mathcal{H}_i|\mathcal{H}_0).\end{aligned}$$

For MPTP scenario, we may also introduce the discrimination probability as

$$\mathrm{P_{dis}} = \sum_{i=0}^{M}\Pr(\mathcal{H}_i|\mathcal{H}_i)\Pr(P_i) = \sum_{i=0}^{M}\Pr(\mathcal{H}_i|\mathcal{H}_i)\Pr(P_i) \tag{28}$$

to describe the performance of power level recognition.

Remark: The definition of $\mathrm{P_{dis}}$ proposed above is alternative. One natural idea is that when power ambiguity appears, the SU randomly select a power level to be the winner instead of directly claiming the failure of power recognition. However, we do not follow this

D. SNR wall

A well known phenomenon in binary spectrum sensing problem is SNR wall effect [25]. In the MPTP scenario, the SNR wall effect can also be observed with slightly modification on the definition of SNR wall. Different from conventional SNR wall that is only related to false alarm and missing detection possibility, SNR wall will be linked with more factors, i.e., multiple decision probability. For each P_k, let us define the following two probabilities:

$$P_{HD}^{(k)} = \sum_{i=k+1}^{M} \Pr(\mathcal{H}_i|\mathcal{H}_k) = \mathcal{Q}\left[\sqrt{N}\left(\frac{\theta_{k+1}}{P_k\gamma + \sigma_k^2} - 1\right)\right], \tag{29}$$

$$P_{LD}^{(k)} = \sum_{i=0}^{k-1} \Pr(\mathcal{H}_i|\mathcal{H}_k) = 1 - \mathcal{Q}\left[\sqrt{N}\left(\frac{\theta_k}{P_k\gamma + \sigma_k^2} - 1\right)\right], \tag{30}$$

where $P_{LD}^{(k)}$ represents the probabilities when the recognized powers are lower than the true power level P_k, while $P_{HD}^{(k)}$ represents the probabilities when the recognized powers are higher than the true power level P_k. Denote the maximal tolerable thresholds for $P_{LD}^{(k)}$ and $P_{HD}^{(k)}$ at SU as two constant values $\mathcal{P}_{LDS}^{(k)}$ and $\mathcal{P}_{HDS}^{(k)}$, respectively. We deem thepower recognition as effective only when the performance meets $P_{LD}^{(k)} \leq \mathcal{P}_{LDS}^{(k)}$ and $P_{HD}^{(k)} \leq \mathcal{P}_{HDS}^{(k)}$.

First we consider the situation where no power ambiguity exists. Since σ_k^2 swings between $\frac{1}{\rho}\sigma_0^2$ and $\rho\sigma_0^2$, the robust detection should satisfies:

$$\mathcal{P}_{HDS}^{(k)} \geq \max_{\sigma_k^2 \in (\frac{1}{\rho}\sigma_0^2, \rho\sigma_0^2)} \left\{\mathcal{Q}\left[\sqrt{N}\left(\frac{\theta_{k+1}}{P_k\gamma + \sigma_k^2} - 1\right)\right]\right\}, \tag{31}$$

$$\mathcal{P}_{LDS}^{(k)} \geq \max_{\sigma_k^2 \in (\frac{1}{\rho}\sigma_0^2, \rho\sigma_0^2)} \left\{1 - \mathcal{Q}\left[\sqrt{N}\left(\frac{\theta_k}{P_k\gamma + \sigma_k^2} - 1\right)\right]\right\}. \tag{32}$$

Since $\mathcal{Q}\left[\sqrt{N}\left(\frac{\theta_{k+1}}{P_k\gamma+\sigma_k^2} - 1\right)\right]$ and $\mathcal{Q}\left[\sqrt{N}\left(\frac{\theta_k}{P_k\gamma+\sigma_k^2} - 1\right)\right]$ are both monotonic increasing function of σ_k^2, we further obtain

$$\mathcal{P}_{HDS}^{(k)} \geq \left\{\mathcal{Q}\left[\sqrt{N}(\frac{\theta_{k+1}}{P_k\gamma + \rho\sigma_0^2} - 1)\right]\right\}, \tag{33}$$

$$\mathcal{P}_{LDS}^{(k)} \geq \left\{1 - \mathcal{Q}\left[\sqrt{N}\left(\frac{\theta_k}{P_k\gamma + \frac{1}{\rho}\sigma_0^2} - 1\right)\right]\right\}. \tag{34}$$

Obviously, the only variable that could be adjusted by SU keep (33) and (34) is the sensing N. It can be directly computed that the sensing time N should satisfy

$$N \geq \max\left\{\left[\frac{\mathcal{Q}^{-1}(\mathcal{P}_{HDS})}{\theta_{k+1}/(P_k\gamma+\rho\sigma_0^2) - 1}\right]^2, \left[\frac{\mathcal{Q}^{-1}(1-\mathcal{P}_{LDS})}{\theta_k/(P_k\gamma+\frac{1}{\rho}\sigma_0^2) - 1}\right]^2\right\}, \tag{35}$$

in order to achieve the robust detection. We could then compute the lower boundary of N from (35). If this lower bound is infinite, then the recognition fails no matter how long the sensing time is. Similar to [25], this phenomenon is named as SNR wall

It is then interesting to derive the conditions under which SNR wall happens such that one can choose the system parameters in the real application to avoid SNR wall. Referring to (**??**), if either of the two formula in the parenthesis is infinite, sample length N must take an infinite value to satisfy the constraint, thus, SNR wall arises.

Since $\mathcal{Q}(\mathcal{P}_{HDS}^{(k)})$ is a constant, $\left[\frac{\mathcal{Q}^{-1}(\mathcal{P}_{HDS})}{\theta_{k+1}/(P_k\gamma+\rho\sigma_0^2)-1}\right]^2$ will go to infinite when its denominator $\frac{\theta_{k+1}}{(P_k\gamma+\rho\sigma_0^2)}-1$ approaches zero, which is expanded as

$$\begin{aligned}\frac{\theta_{k+1}}{P_k\gamma+\rho\sigma_0^2}-1 &= \frac{P_{k+1}\gamma+\frac{1}{\rho}\sigma_0^2}{(P_{k+1}\gamma+\frac{1}{\rho}\sigma_0^2)-(P_k\gamma+\rho\sigma_0^2)}\ln\left(\frac{P_{k+1}\gamma+\frac{1}{\rho}\sigma_0^2}{P_k\gamma+\rho\sigma_0^2}\right)-1 \\ &= \frac{P_{k+1}\gamma+\frac{1}{\rho}\sigma_0^2}{((P_{k+1}\gamma-P_k)-(\rho\sigma_0^2-\frac{1}{\rho}\sigma_0^2)}\ln\left[1+\frac{(P_{k+1}\gamma-P_k)-(\rho\sigma_0^2-\frac{1}{\rho}\sigma_0^2)}{P_k\gamma+\rho\sigma_0^2}\right]-1. \end{aligned} \tag{36}$$

Here we prove that (36) approaches zero when $(P_{k+1}-P_k)\gamma$ drops from infinite to $\rho\sigma_0^2-\frac{1}{\rho}\sigma_0^2$. For easier explanation, we denote $(P_{k+1}-P_k)\gamma-(\rho\sigma_0^2-\frac{1}{\rho}\sigma_0^2)$ by A. According to $\ln(1+x)\sim O(x)$, (36) there is:

$$\lim_{A\to 0}\left\{\frac{P_{k+1}\gamma+\sigma_L^2}{A}\ln\left[1+\frac{A}{P_k\gamma+\rho\sigma_0^2}\right]-1\right\}=\frac{P_{k+1}\gamma+\sigma_L^2}{A}\frac{A}{P_k\gamma+\rho\sigma_0^2}-1=0. \tag{37}$$

In turn, we have the conclusion that $\left[\frac{\mathcal{Q}^{-1}(\mathcal{P}_{HDS})}{\theta_{k+1}/(P_k\gamma+\rho\sigma_0^2)-1}\right]^2$ has an infinite value when $(P_{k+1}-P_k)\gamma=\rho\sigma_0^2-\frac{1}{\rho}\sigma_0^2$ stands.

Similarly, we can prove that when $(P_k-P_{k-1})\gamma-(\rho\sigma_0^2-\frac{1}{\rho}\sigma_0^2)$ approaches zeros, $\left[\frac{\mathcal{Q}^{-1}(1-\mathcal{P}_{LD})}{\theta_k/(P_k\gamma+\frac{1}{\rho}\sigma_0^2)-1}\right]^2$ approaches infinite too.

Before formulating the position of SNR wall, define a new variable: $\Delta\text{SNR}_{(k)}\triangleq\frac{(P_{k+1}-P_k)\gamma}{\sigma_0^2}$. Rewrite $(P_{k+1}-P_k)\gamma\to(\rho-\frac{1}{\rho})$ as $\Delta\text{SNR}_{(k)}\to(\rho-\frac{1}{\rho})$, it is known that when $\Delta\text{SNR}_{(k)}$ approaches $\rho-\frac{1}{\rho}$, the required sensing time to achieve accurate recognition increases till infinite. Thus, $\rho-\frac{1}{\rho}$ is defined as the position of SNR wall. Fig. 4 displays SNR walls on three different locations caused by different sizes of noise uncertainty. It is also seen that the required sensing time increases more sharply as $\Delta\text{SNR}_{(k)}$ approaches $\rho-\frac{1}{\rho}$.

Now, consider the condition where the real $\Delta\text{SNR}_{(k)}$ drops below the SNR wall threshold. It is not hard to note that with ρ gets larger, the performance is worse. Besides, it worth notice that the SNR wall threshold is coincidentally the boundary condition for power ambiguity to arise. Thus, increase of ρ could result in power ambiguity, which directly impairs the detection performance.

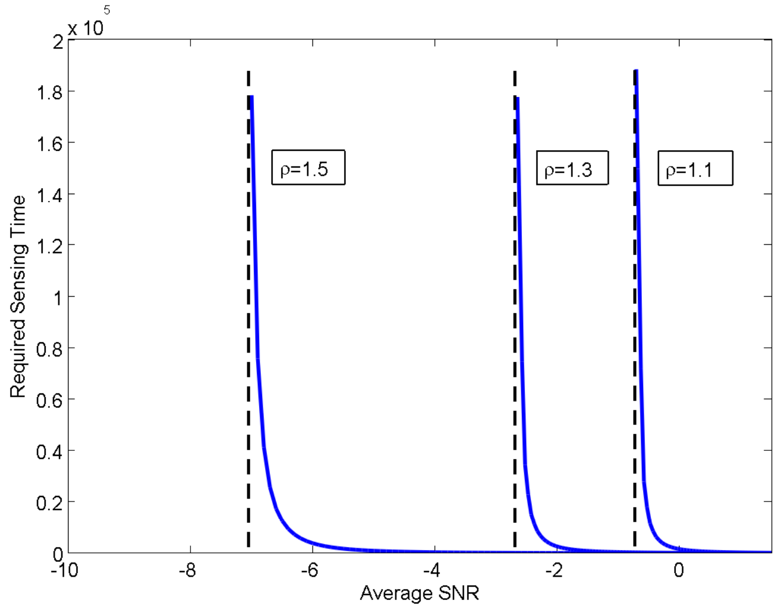

Fig. 4. The position of SNR wall when noise uncertainty is of different size.

Thus, the performance becomes even worse, so we say the recognition fails regardless of the sensing time. Hence, For any k, $\rho - \frac{1}{\rho}$ is the minimum value of $\Delta\text{SNR}_{(k)}$ when recognition is accurate. To achieve accurate recognition, the set of power levels at PU should comply to both of these two restrictions:

$$\Delta\text{SNR}_{(k)} \geq \rho - \frac{1}{\rho}, \tag{38}$$

$$\Delta\text{SNR}_{(k-1)} \geq \rho - \frac{1}{\rho}. \tag{39}$$

When either $\Delta\text{SNR}_{(k)}$ or $\Delta\text{SNR}_{(k-1)}$ is lower than SNR wall, the recognition fails.

Let us summarize the effects of SNR wall as follows:

1) When the gap between power levels $\gamma(P_k - P_{k-1})$ or $\gamma(P_{k+1} - P_k)$ approaches SNR wall, the required sensing time for correct recognition increases.
2) When the gap between power levels $\gamma(P_k - P_{k-1})$ or $\gamma(P_{k+1} - P_k)$ is lower than SNR wall, the recognition fails.

Remark 3: Researchers should always pay attention to the derivation of the location of SNR wall is based on extreme cases, or more exactly, cases where the given SU has the worst recognition performance. The sense of keeping away from SNR wall is to guarantee the detection satisfies our preset requirements in all cases. Thus, in real detection or Matlab-based simulation, it is possible that even though the ΔSNR is below SNR wall, the performance is still acceptable.

Remark 4: Although the restriction for power levels here are different from classic SNR wall, they have consistent physical sense. SNR wall sets restrictions on the power gap between each power level and its two neighbours. The value of ρ represents the size of noise uncertainty at SU. Different sizes of noise uncertainty will construct SNR walls on different positions, as shown in Fig.4. If noise uncertainty decreases, the position of SNR wall will be pushed back. When noise variance is a certain value, the SNR wall will be pushed back infinitely, i.e., SNR wall disappears. Traditional CR has only two power levels: $P_0 = 0$ and $P_1 = P$, to evade SNR wall, $(P_1 - P_0)$ is attached with restriction, which is a special case for our MPTP scenario.

Remark 5: The SNR wall phenomenon and power ambiguity has something in common, that is, the position of SNR wall is coincidental to the critical condition of power ambiguity. Both of these two phenomena are caused by noise uncertainty, so naturally, we do studies on the potential relationship between these two phenomena.

The mean value of decision statistics $T(\mathbf{x})$ when PU transmits by P_k is $\gamma P_k + \sigma_k^2$, whose value possibly drops in the ambiguity area between P_k and P_{k+1} or P_{k-1}. And pay attention to the variance of $T(\mathbf{x})$ keeps decreasing along with the increase of sensing time, infinite sensing time is equivalent to zero variance. According to the features of Gaussian distribution, if the variance is small enough, it is fair to declare that its value is restricted within a small range centered by its mean value. Thus, if the mean value of $T(\mathbf{x})$ unfortunately falls in the ambiguity area, increasing sensing time even impairs the detection performance, rather than counteracts the effects brought by noise uncertainty.

Hence, we could conclude that when power ambiguity exists, SNR wall also exists, but this conclusion cannot be exchanged.

Remark 6: Since $(P_{k+1} - P_k)$ differs for different k, it is possible that some power levels could satisfy the requirements in (38) (39), while the others cannot. Hence, we could divide the power levels into two groups as shown in Fig. **??**, where the power levels on the right side of

SNR wall meet (38) and (39), while the power levels on the left side do not. A special case is that gaps between any two neighboring power levels are the same i.e.

$$P_{i+1} - P_i = \text{Constant} \qquad i = 0, 1, ..., M-1. \tag{40}$$

In this case, we could eliminate the subscript of ΔSNR_k since the set $\{\Delta\text{SNR}_k | k \in \{0, 1, ..., M-1, M\}\}$ has a single value.

IV. Cooperative Spectrum Sensing via Majority Voting

In this section we examine the distributed cooperative spectrum sensing, where K SUs cooperate to detect the presence of PU as well as the power levels by forwarding their decision results $\{0, \ldots, M\}$ to a fusion center. The conventional fusion rules, e.g., AND, OR, and KON rules [20] are defined on the binary decision while not applicable for MPTP scenario. In [20], a new fusion method based on the majority rule was proposed by locating the power levels that are claimed the most times by the SUs.

However, when the noise variance contains the uncertainty, the method in [20] cannot be directly applied because the decisions made by one SU-k may contain one or more power levels due to power ambiguity, and the sensing is likely to fail due to the existence of SNR walls. Fortunately, section III-B shows that the power ambiguity only happens among contiguous power level. The application of cooperative sensing is then very hopeful to counteract the power ambiguity since different SUs might vote for different bunches of power levels and the selection probability of the true one is greatly enhanced. To better illustrate the proposed cooperative sensing scheme, we assume that that power ambiguity at each SU only happens between two neighboring power levels, while extension to more complicated situations is straightforward.

The fusion center build a $K \times (M+1)$ matrix $\mathbf{A} = [\vec{a}_1, \vec{a}_2, \cdots, \vec{a}_K]^T$ based the decisions from all K SUs, where $\vec{a}_k = (a_{k1}, \cdots, a_{k(M+1)})$ denotes the k-th SU's decision for all $M+1$ power levels. The element $a_{kj} = 1$ denotes that the k-th SU vote for P_{j-1}, otherwise $a_{kj} = 0$. Moreover, let us formulate a voting pool $\vec{d} = (d_0, \cdots, d_M)$, where d_m denotes the number of SUs that claim $\mathcal{H}_m$. For a given $\mathbf{A}$, there is

$$d_m = \sum_{i=1}^{K} a_{i(m+1)}, \forall m \in \{0, \cdots, M\}. \tag{41}$$

Moreover define $D=\sum_{m=0}^{M} d_m=\sum_{i=1}^{K}\sum_{j=1}^{M+1} a_{ij}$ as the total number of hypotheses that all the SUs claim. Obviously, there is $K \leq D \leq 2K$ due to our previous assumption. We also need to introduce a $(2M+1)\times 1$ vector $\vec{c}=(c_0,\cdots,c_M,c_{0,1},c_{1,2},\ldots,c_{M-1,M})$ to compute the probability of $\vec{d}$, where c_i denotes the number of SUs that claim only one power level P_i, while $c_{i,i+1}$ denotes the number of SUs that claim both power levels P_i, P_{i+1}. Obviously, there is $\sum_{i=0}^{M} c_i+\sum_{i=0}^{M-1} c_{i,i+1}=K$.

Once gain, in order to provide a concise illustration we assume that each SU has the same decision probabilities $\Pr(\mathcal{H}_j|\mathcal{H}_i)$ and $\Pr(\mathcal{A}_{j,j+1}|\mathcal{H}_i)$. Then, the probability of any specific $\vec{c}$ can be computed as

$$\begin{aligned}\Pr(\vec{c}|\mathcal{H}_k) &= \binom{K}{c_0}\Pr(\mathcal{H}_0|\mathcal{H}_k)^{c_0}\binom{K-c_0}{c_1}\Pr(\mathcal{H}_1|\mathcal{H}_k)^{c_1}\cdots \\ &\quad \binom{K-\sum_{l=0}^{M-1} c_l}{c_M}\Pr(\mathcal{H}_M|\mathcal{H}_k)^{c_M}\binom{K-\sum_{l=0}^{M} c_l}{c_{0,1}}\Pr(\mathcal{H}_{0,1}|\mathcal{H}_k)^{c_{0,1}}\cdots \\ &\quad \binom{K-\sum_{l=0}^{M} c_l-\sum_{i=0}^{M-2} c_{i,i+1}}{c_{M-1,M}}\Pr(\mathcal{H}_{M-1,M}|\mathcal{H}_k)^{c_{M-1,M}} \\ &= \frac{K!}{\prod_{l=0}^{M} c_l!\prod_{i=0}^{M-1} c_{i,i+1}!}\prod_{m=0}^{M}\Pr(\mathcal{H}_m|\mathcal{H}_k)^{c_m}\prod_{u=0}^{M-1}\Pr(\mathcal{H}_{u,u+1}|\mathcal{H}_k)^{c_{u,u+1}}.\end{aligned} \tag{42}$$

Proposition 1: The probability of a given $\vec{d}$ under $\mathcal{H}_i$ could be mapped from a series of $\vec{c}$. Before giving the form of mapping function, we propose a lemma.

Lemma 2: For a given $\vec{d}$, the degree of freedom for $\vec{c}$ is M instead of the primal (2M+1).

Proof: It is obvious that $\vec{d}$ and $\vec{c}$ have the following mapping relationship:

$$d_i=\begin{cases} c_0+c_{0,1}, & i=0 \\ c_i+c_{i-1,i}+c_{i,i+1}, & 1\leq i\leq M-1 \\ c_M+c_{M-1,M}, & i=M. \end{cases} \tag{43}$$

Assume that $c_0,c_1,\cdots,c_{M-1}$ are known, then $c_{0,1}$ is determined by the equation $c_{0,1}=d_0-c_0$. Further, $c_{1,2}$ is determined since $c_{0,1}+c_1+c_{1,2}=d_1$. The conclusion of $c_{1,2}$ could be easily extended to $c_{i,i+1}$, where $i<M$. Finally, c_M is determined by $c_M=d_M-c_{M-1,M}$.

$c_{m-1,m}$ can be obtained by mathematical induction

$$c_{m-1,m}=(-1)^{m-1}\sum_{n=0}^{m-1}(-1)^n(d_n-c_n). \tag{44}$$

■

Now, we give the mapping function form $\vec{c}$ to $\vec{d}$ as the follows:

$$\Pr(\vec{d}|\mathcal{H}_i) = \sum_{c_0=0}^{d_0} \sum_{c_1=\max\{0,l_1\}}^{\min\{d_1,u_1\}} \cdots \sum_{c_m=\max\{0,l_m\}}^{\min\{d_m,u_m\}} \cdots \sum_{c_{M-1}=\max\{0,l_{M-1}\}}^{\min\{d_{M-1},u_{M-1}\}} \Pr(\vec{c}|\mathcal{H}_i), \tag{45}$$

where c_0 must satisfy $\sum_{i=0}^{M} c_i + \sum_{i=0}^{M-1} c_{i,i+1} = K$, and u_m, l_m are defined as

$$\begin{cases} u_m = d_m + (-1)^m \sum\limits_{n=0}^{m-1} (-1)^n (d_n - c_n) \\ l_m = -d_{m+1} + u_m \end{cases} \quad m = 1, 2, \cdots, M-1. \tag{46}$$

Proof:

According to Lemma 2,we could only determine the value of $c_0, c_1, \cdots, c_{M-1}$ to completely determine a $\vec{c}$, so the summation has only M summation signs. We Assume c_0 ranges from 0 to d_0. After c_0 being determined, $c_{0,1}$ is determined as a result of $c_0 + c_{0,1} = d_0$. Then from the condition $c_1 + c_{0,1} + c_{1,2} = d_1$ we obtain $c_{1,2} = d_1 - c_1 - c_{0,1}$, which must satisfy

$$0 \le c_{1,2} = d_1 - c_1 - c_{0,1} \le d_2,$$

or equivalently that c_1 must satisfy

$$-d_2 + d_1 - d_0 + c_0 \le c_1 \le d_1 - d_0 + c_0.$$

After the range of c_1 is determined, the range of $c_{1,2}$ can also be determined. Similarly when the range of c_{m-1} is determined, the range of $c_{m-1,m}$ is also determined, and $c_{m,m+1} = d_m - c_m - c_{m-1,m}$ must satisfy

$$0 \le c_{m,m+1} = d_m - c_m - c_{m-1,m} \le d_{m+1},$$

which gives

$$-d_{m+1} + d_m - c_{m-1,m} \le c_m \le d_m - c_{m-1,m}.$$

Where $c_{m-1,m}$ is given in 44. Meanwhile, considering $0 \le c_m \le d_m$, we obtain the upper and lower bounds of c_m as shown in (45). The proof is completed. ■

In the fusion center, the power level corresponding to the largest value in $\vec{d}$ will win out:

$$\hat{m} = \arg\max_{m \ge 0} \ d_m. \tag{47}$$

A special case may happen when more than one $\hat{m}$ achieve the maximum votes. In this case we say that power ambiguity arises, and the recognition is claimed to fail.

Define $\Pr_m(\mathcal{H}_j|\mathcal{H}_i)$ as the decision probability. Pay attention to our recognition strategy in the fusion center is different from [20] as we directly apply recognition here rather than first implement an on-off detection. In our scenario, $\Pr_m(\mathcal{H}_j|\mathcal{H}_i)$ can be computed as

$$\Pr_m(\mathcal{H}_j|\mathcal{H}_i) = \sum_{d_j=\lceil \frac{D}{M} \rceil}^{\lfloor \frac{D}{2} \rfloor} \sum_{d_0=\max\{0,\alpha_0\}}^{\min(d_j,\beta_0)} \sum_{d_1=\max\{0,\alpha_1\}}^{\min\{d_j,\beta_1\}} \cdots \sum_{d_M=\max\{0,\alpha_M\}}^{\min\{d_j,\beta_M\}} \Pr(\vec{d}|\mathcal{H}_i) \tag{48}$$

where $\lfloor \cdot \rfloor$ and $\lceil \cdot \rceil$ denote the ceiling function and floor function, respectively. Moreover, α and β are defined as

$$\begin{aligned} \alpha_m &= \begin{cases} D - \sum_{i=0}^{m-1} d_i - (M-m+1)d_j, & 1 \le m < j \\ D - \sum_{i=0}^{m-1} d_i - (M-m)d_j, & j < m \le M \end{cases} \\ \beta_m &= \begin{cases} D - \sum_{i=0}^{m-1} d_i - d_j, & 1 \le m < j \\ D - \sum_{i=0}^{m-1} d_i, & j < m \le M \end{cases} \end{aligned} \tag{49}$$

It is expected that $\Pr_m(\mathcal{H}_i|\mathcal{H}_i)$ is larger than $\Pr(\mathcal{H}_i|\mathcal{H}_i)$ due to the cooperative sensing. However, it is not easy to prove that in mathematics due to the complexity of 48, so we will prove that by computer-based simulation in the next section.

V. SIMULATIONS

In this section we provide simulation results to evaluate the performance of the proposed spectrum sensing algorithms. Define the average SNR in MPTP scenario as $\text{SNR}_{av} = \sum_{i=1}^{M} \Delta\text{SNR}_i \Pr(\mathcal{H}_i)$. Four positive power levels are assumed for PU, and the prior probabilities of all $\mathcal{H}_i$'s, $i \ge 0$, are set as 0.5, 0.2, 0.125, 0.075, 0.1, respectively.

We first demonstrate the sensing performance for both the detection probability and the discrimination probability versus the average SNR in Fig. 5. The number of the sensing sample is taken as $N = 6000$. It is seen that the spectrum sensing suffers from slight discrimination performance loss due to the noise power uncertainty. However, the detection probability is higher when $\rho = 1.2$. The reason is that the threshold θ_k in (20) decreases when ρ increases, forcing

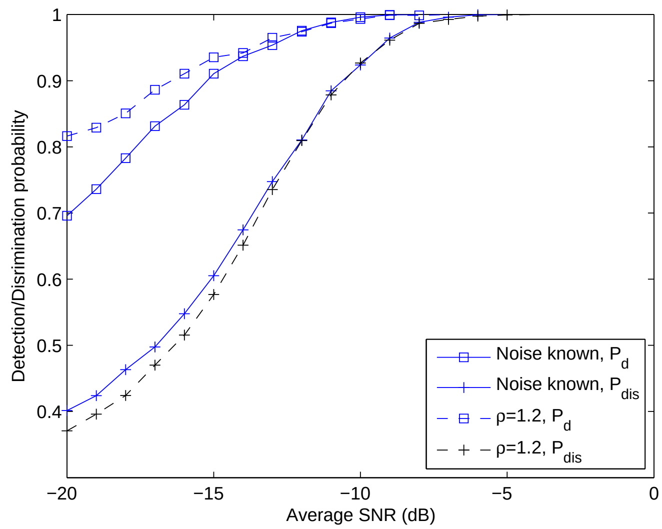

Fig. 5. Detection and discrimination probability for noise known and uncertainty condition versus average SNR with $N = 6000$.

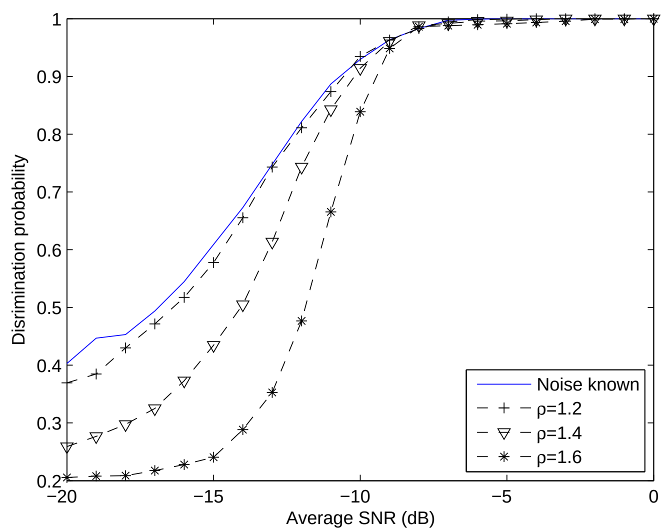

Fig. 6. Discrimination probability versus average SNR for various ρ with $N = 6000$.

the detector to prefer higher power level. Thus the false alarm probability becomes pretty high when ρ increases.

Fig. 6 evaluates the discrimination performance versus the average SNR for various ρ. The number of the sensing sample is taken as $N = 6000$. It is seen that the discrimination performance

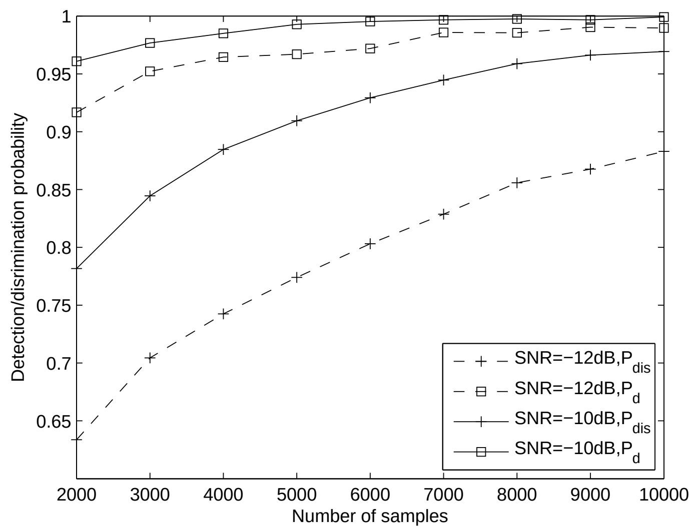

Fig. 7. Detection and discrimination probability versus the number of samples with $\rho = 1.2$.

degrades when ρ increases, which reflects that the noise uncertainty could seriously affect the discrimination performance at low SNR. Indeed the thresholds $\theta_k, k = 0, 1, \cdots, M+1$ are important for discriminating power level. The thresholds obtained from noise power known condition are optimal, we can demonstrate the best discrimination performance. When the uncertainty increases, the thresholds become far away from the optimal. Specifically, when $\rho = +\infty$, the detector could not discriminate power level any more, as mentioned in Section III-A.

We then evaluate both the detection probability and discrimination probability versus the number of samples in Fig. 7. The average SNR is taken as -10 dB and -12 dB respectively. The energy detection approach requires large number of samples to obtain good performance. It is seen that a long sensing period could reduce the effect of noise uncertainty.

Wealso provide the simulation to demonstrate the impacts of SNR wall in Fig. 8, where. where the worst discrimination performance with different sizes of noise uncertainty. It is seen that when noise uncertainty is lighter, longer sensing period could guarantee better performance. However, when the real ΔSNR approaches the location of , extending sensing time is helpless. Specially, when ΔSNR is exactly at the value of SNR wall, no gains would be observed by

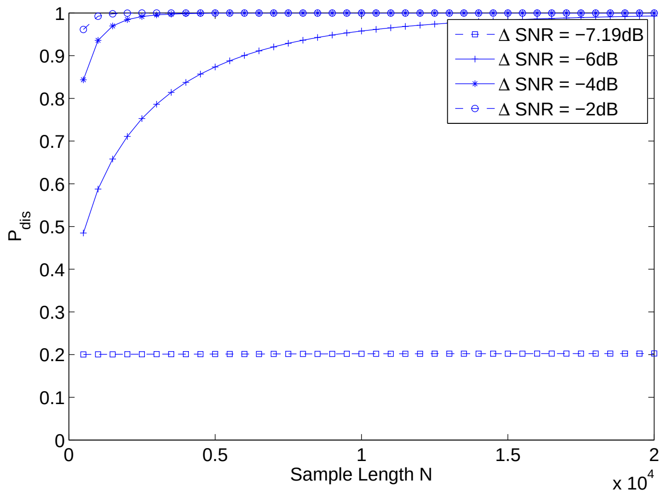

Fig. 8. The worst discrimination performance versus sensing time under different sizes of noise uncertainty.

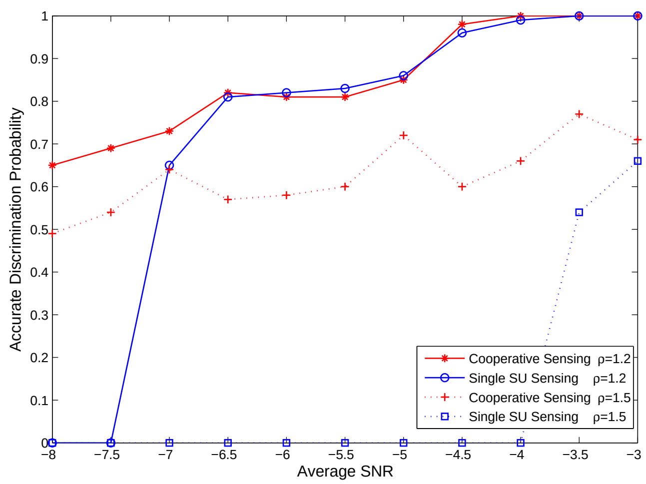

Fig. 9. The discrimination performance versus average SNR when 200 SUs cooperate and one SU works alone under different sizes of noise uncertainty.

increasing the sensing time, which matches our theoretical studies very well.

Lastly, we compare the performance of cooperative sensing scheme and the individual sensing in Fig. 9. The number of the received sampling is It is observed that when SNR is very low, sensing by only one SU can hardly obtain acceptable performance . In some worst cases, the discrimination accuracy even approaches zero, while the cooperative sensing can still give satisfactory result. Nevertheless, when the SNR becomes larger the performance of a single SU improves fast. It is shown that the curve of single sensing approaches asymptotically to the curve of cooperative sensing.

VI. Conclusions

In this paper, we studied the spectrum sensing in MPTP scenario under noise uncertainty. The GLRT paradigm is used to estimate the noise variance, and a method is derived to discriminate the primary transmitting power level. For energy detection approach if the noise variance is limited in an appropriate range, an accurate primary transmit power could be sensed by the SU. Detection and discrimination performance are analyzed to associated with the quantity of uncertainty and the number of samples. Thresholds derived in closed-form are strongly related to the quantity of uncertainty hence the discrimination performance is sensitive about noise power uncertainty. Specially, the SNR wall phenomena is investigated and formulated. Moreover, one cooperative sensing strategy called MMDF is proposed and confirmed to obtain better recognition by simulation results.

References

[1] S. Haykin, "Cognitive radio: brain-empowered wireless communications," *Selected Areas in Communications, IEEE Journal on*, vol. 23, no. 2, pp. 201–220, 2005.

[2] S. Haykin, D. Thomson, and J. Reed, "Spectrum sensing for cognitive radio," *Proceedings of the IEEE*, vol. 97, no. 5, pp. 849–877, 2009.

[3] A. Sahai and D. Cabric, "Spectrum sensing: fundamental limits and practical challenges," in *Proc. IEEE International Symposium on New Frontiers in Dynamic Spectrum Access Networks (DySPAN)*, 2005.

[4] H.-S. Chen, W. Gao, and D. Daut, "Signature based spectrum sensing algorithms for ieee 802.22 wran," in *Communications, 2007. ICC '07. IEEE International Conference on*, June 2007, pp. 6487–6492.

[5] D. Cabric, S. Mishra, and R. Brodersen, "Implementation issues in spectrum sensing for cognitive radios," in *Signals, Systems and Computers, 2004. Conference Record of the Thirty-Eighth Asilomar Conference on*, vol. 1, Nov 2004, pp. 772–776 Vol.1.

[6] P. Sutton, K. Nolan, and L. Doyle, "Cyclostationary signatures in practical cognitive radio applications," *Selected Areas in Communications, IEEE Journal on*, vol. 26, no. 1, pp. 13–24, Jan 2008.

[7] A. Ghasemi and E. Sousa, "Spectrum sensing in cognitive radio networks: requirements, challenges and design trade-offs," *Communications Magazine, IEEE*, vol. 46, no. 4, pp. 32–39, 2008.

[8] R. Tandra and A. Sahai, "Fundamental limits on detection in low snr under noise uncertainty," in *Wireless Networks, Communications and Mobile Computing, 2005 International Conference on*, vol. 1, June 2005, pp. 464–469 vol.1.

[9] W. Lin and Q. Zhang, "A design of energy detector in cognitive radio under noise uncertainty," in *Communication Systems, 2008. ICCS 2008. 11th IEEE Singapore International Conference on*, 2008, pp. 213–217.

[10] T. J. Lim, R. Zhang, Y. C. Liang, and Y. Zeng, “GLRT-based spectrum sensing for cognitive radio,” in *Global Telecommunications Conference, 2008. IEEE GLOBECOM 2008. IEEE*, Nov 2008, pp. 1–5.

[11] J. Font-Segura and X. Wang, “GLRT-based spectrum sensing for cognitive radio with prior information,” *Communications, IEEE Transactions on*, vol. 58, no. 7, pp. 2137–2146, 2010.

[12] I. . L. S. Committee *et al.*, “Wireless lan medium access control (mac) and physical layer (phy) specifications,” *IEEE Standard*, vol. 802, no. 11, 1999.

[13] 3GPP TS 36.213, Evolved Universal Terrestrial Radio Access (EUTRA), “User Equipment (UE) Radio Transmission and Reception,”(release 8).

[14] 3GPP TR 36.913, “Requirements for Further Advancements for Evolved Universal Terrestrial Radio Access (E-UTRA) (LTE-Advanced),” 3GPP, Tech. Rep. v. 10.0.0, Mar. 2011.

[15] Z. Chen, F. Gao, X. Zhang, J. Li, and M. Lei, “Sensing and power allocation for cognitive radio with multiple primary transmit powers,” *Wireless Communications Letters, IEEE*, vol. 2, no. 3, pp. 319–322, 2013.

[16] Tandra R, Sahai A. Fundamental limits on detection in low SNR under noise uncertainty[C]//Wireless Networks, Communications and Mobile Computing, 2005 International Conference on. IEEE, 2005, 1: 464-469. MLA

[17] Poor V, Looze D P. Minimax state estimation for linear stochastic systems with noise uncertainty[J]. Automatic Control, IEEE Transactions on, 1981, 26(4): 902-906.

[18] Oude Alink M S, Kokkeler A B J, Klumperink E A M, et al. Lowering the SNR wall for energy detection using cross-correlation[J]. Vehicular Technology, IEEE Transactions on, 2011, 60(8): 3748-3757.

[19] Mariani A, Giorgetti A, Chiani M. SNR wall for energy detection with noise power estimation[C]//Communications (ICC), 2011 IEEE International Conference on. IEEE, 2011: 1-6.

[20] Gao F, Li J, Jiang T, et al. Sensing and Recognition When Primary User Has Multiple Transmit Power Levels[J]. Signal Processing, IEEE Transactions on, 2015, 63(10): 2704-2717.

[21] S. Shelhammer and G. Chouinard, “Spectrum sensing requirements summary,” IEEE P802.22-06/0089r1, Tech. Rep., June 2006.

[22] D. Torrieri, “The radiometer and its practical implementation,” in *2010 Military Communication Confrence*, pp.304–310, 2010.

[23] S. M. Kay, *Fundamentals of Statistical signal processing, Volume 2: Detection theory*. Prentice Hall PTR, 1998.

[24] S. S. Wilks, *Mathematical Statistics*. Read Brooks, 2007.

[25] R. Tandra and A. Sahai, “SNR walls for signal detection,” *Selected Topics in Signal Processing, IEEE Journal of*, vol. 2, no. 1, pp. 4–17, 2008.

[26] Y.-C. Liang, Y. Zeng, E. Peh, and A. T. Hoang, “Sensing-throughput tradeoff for cognitive radio networks,” *Wireless Communications, IEEE Transactions on*, vol. 7, no. 4, pp. 1326–1337, 2008.

[27] 3GPP TS 36.213, Evolved Universal Terrestrial Radio Access (EUTRA), “User Equipment (UE) Radio Transmission and Reception,”(release 8).

[28] 3GPP TR 36.913, “Requirements for Further Advancements for Evolved Universal Terrestrial Radio Access (E-UTRA) (LTE-Advanced),” 3GPP, Tech. Rep. v. 10.0.0, Mar. 2011.

[29] Y.-C. Liang, Y. Zeng, C. lY. Peh, and A. T. Hoang, “Sensing-throughput tradeoff for cognitive radio networks,” *IEEE Trans. Wireless Commun.*, vol. 7, no. 3, pp. 1326–1337, Mar. 2008.

[30] S.-Q. Liu, B.-J. Hu, and X.-Y. Wang, “Hierarchical cooperative spectrum sensing based on double thresholds energydetection,” *IEEE Commun. Lett.*, vol. 16, pp. 1096–1099, 2012.

[31] K. Zhang, J. Li, and F. Gao, “Machine learning techniques for spectrum sensing when primary user has multiple transmit power,” in *IEEE Int. Conf. Commun. Sys. (ICCS)*, Nov. 2014, Macau, China, pp. 137–141.